Hydrometallurgy 220 (2023) 106107

Contents lists available at ScienceDirect

Hydrometallurgy

journal homepage: www.elsevier.com/locate/hydromet

Streamline-based reactive transport modeling of uranium mining during in-situ leaching: Advantages and drawbacks

Maksat B. Kurmanseiit [a,b,*], Madina S. Tungatarova [a,b,*], Jean-Jacques Royer [c], Daniar Y. Aizhulov [d], Nurlan M. Shayakhmetov [b], Aidarkhan Kaltayev [a]

[a] Department of Mechanical Engineering, Satbayev University, Almaty 050013, Kazakhstan
[b] Department of Mechanics, Al-Farabi Kazakh National University, Almaty 050040, Kazakhstan
[c] Laboratoire GeoRessources, Université de Lorraine/CNRS, 54000 Nancy, France
[d] Department of Software Engineering, Satbayev University, Almaty 050013, Kazakhstan

ARTICLE INFO

Keywords:
In-situ leaching
Reactive transport model
Streamlines
3D modeling
Uranium recovery

ABSTRACT

Reactive transport modeling is known to be computationally intensive when applied to 3D problems. Transforming sequential computing on the computer processor units (CPU) into parallelized computation on the high-performance parallel graphic processor units (GPU) is a classical approach to increasing computational performance. Another complementary approach is to decompose a complex 3D modeling problem into a set of simpler 1D problems using streamline approaches which can be easily parallelized, therefore reducing computation time. This paper investigates solutions to the equations governing dissolution and transport using streamlines coupled with a parallelization approach. In addition, an analytical solution to the dissolution and transfer equations of uranium describing the In-Situ Leaching (ISL) mining recovery is found using an approximation series to the 2nd order. The analytical solution is compared to the 1D numerical resolution along the streamlines and to the 3D simulation results superimposed on the streamline. Both approaches give similar results with a relative error of <2 % (2%). The proposed methodology is then applied to a case study in which the classical 3D resolution is compared to the newly suggested streamline solution, demonstrating that the streamline approach increases computational performances by a factor ranging from hundred to thousand depending on the complexity of the grid-block model.

1. Introduction

In-Situ Leaching (ISL) is a common method used to recover minerals in the mining industry, particularly for uranium deposits such as those exploited in Kazakhstan (Uranium Production by Country, 2022; Bruneton and Cuney, 2016; International Atomic Energy Agency, 2009). Given the geological/ mineralogical heterogeneity of deposits, and the complexity of the physicochemical processes involved during the leaching of minerals by the ISL method, the dissolution/precipitation modeling of compounds is computationally resource-intensive, specifically for 3D modeling. However, the number of mineable uranium deposits mined at a cost of less than USD 80 per kilogram is currently decreasing, requiring an efficient non-expensive optimization modeling approach to better extract the commodities. According to the Organization for Economic Co-operation and Development (OECD) (OECD, 2020; OECD, 2008), the number of such "easily" mineable resources decreased by as much as 55% during these last 15 years, and only about 2.0 million tons of such uranium deposits are currently available for mining (OECD, 2020). Currently, deeper low grade mineralized layers must be exploited; their ore quality decreases as they are characterized by lower amounts of fine- to medium-grained size sandstone enriched with often clay minerals (montmorillonite, smectite, and illite). Therefore, there is a need to conduct more detailed analyses of both geological modeling and geotechnological test-site and production modes in the field. Thus, an increase in the performance of calculations is required to conduct this detailed analysis. It can be achieved by using high-performance intensive calculation methods such as performing calculations on the graphics processor unit (GPU) instead of the classical computer processor unit (CPU). In addition, if calculations can be easily parallelized such that the full GPU performance can be used, the reduction in the amount of calculations required will be significant. The streamlines approach presents several advantages: it transforms a three-

* Corresponding authors at: Department of Mechanical Engineering, Satbayev University, Almaty 050013, Kazakhstan.
E-mail addresses: m.kurmanseiit@satbayev.university (M.B. Kurmanseiit), m.tungatarova@satbayev.university (M.S. Tungatarova).

https://doi.org/10.1016/j.hydromet.2023.106107
Received 4 January 2023; Received in revised form 22 June 2023; Accepted 24 June 2023
Available online 29 June 2023
0304-386X/© 2023 The Authors. Published by Elsevier B.V. This is an open access article under the CC BY license (http://creativecommons.org/licenses/by/4.0/).

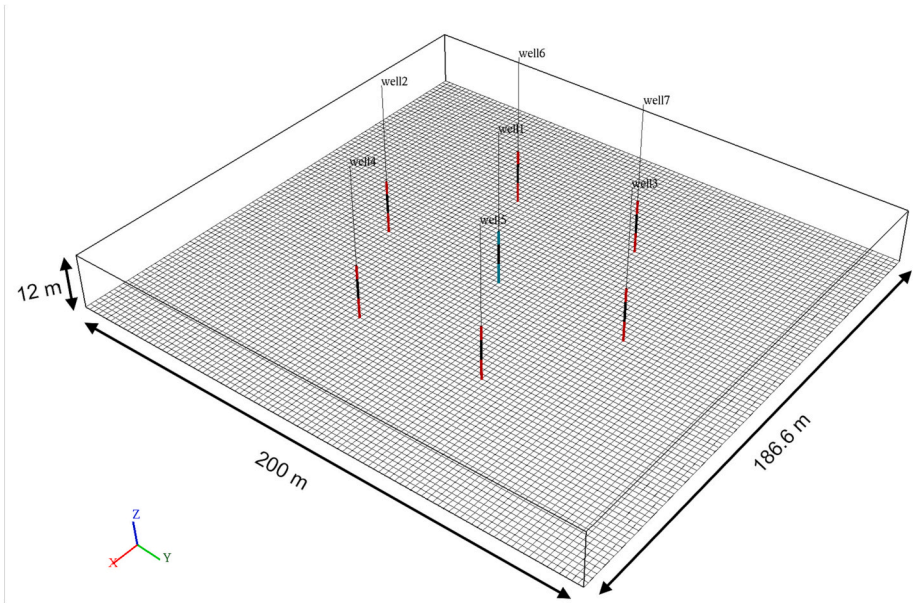

Fig. 1. Computational domain for modeling fluid flow in an ISL mining operation with a hexagonal well pattern.

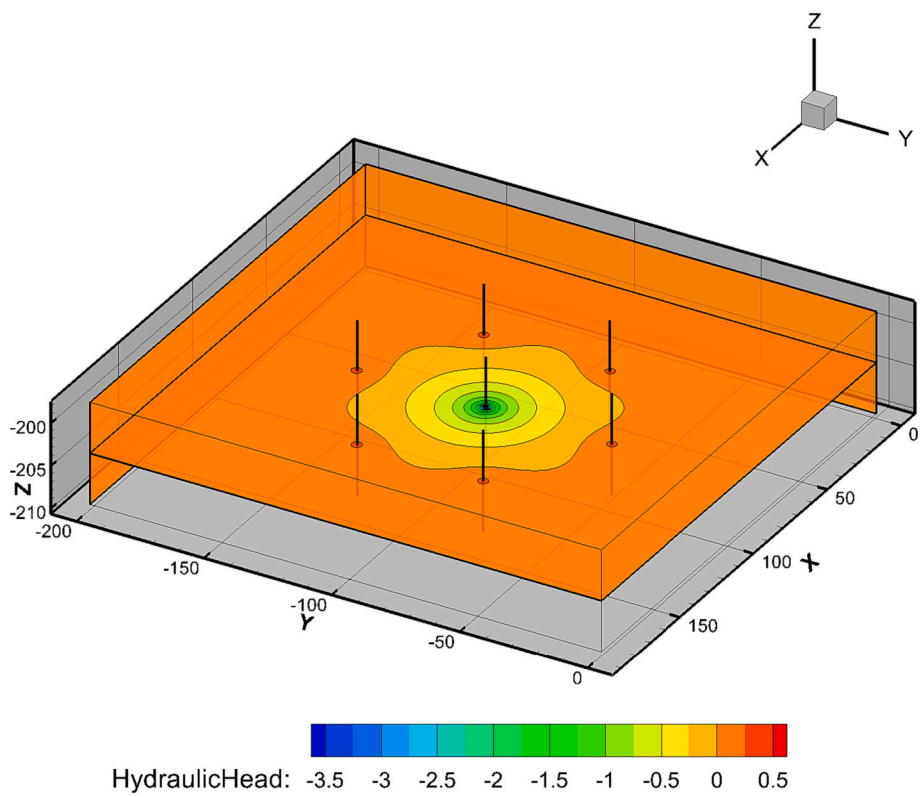

Fig. 2. Modeling of the the pressure field in an ISL mining exploitation with a hexagonal well pattern.

dimensional problem into a set of simplified one-dimensional parallelizable equations that can be solved along the streamlines. Historically, 1D numerical solutions along streamlines were first introduced by Bommer and Schechter (1979) (Bommer and Schechter, 1979) to solve a uranium leaching problem. Since this early paper, several works have investigated modeling in-situ uranium leaching including 1D, 2D, and 3D models (Gromov, 1978; Grenthe et al., 2004; Zheng and Wang, 1999; Kuljabekov, 2014; Panfilov et al., 2016; Aizhulov et al., 2022).

This study discusses the In-Situ Leaching (ISL) method used in uranium mining in Kazakhstan and the need for increased computational efficiency in modeling the complex physicochemical processes involved in mineral leaching. The article proposes solutions to the dissolution/transport equations for the ISL process using streamlines coupled with a parallelization approach on a hexagonal well pattern. Additionally, it presents a novel analytical solution to the uranium dissolution and transfer equations in ISL mining, which is compared to 1D numerical resolution and 3D simulation results. The study emphasizes the importance of improving computational efficiency to meet the

Table 1
Thermodynamic data of some uranium species.

Label	Species[1]	$\Delta_f G_m^0$ (kJ mol^{-1})	$\Delta_f H_m^0$ (kJ mol^{-1})	S_m^0 (J mol^{-1} K^{-1})
M	$UO_{3(s)}$	−1145.7 ± 1.2	−1224 ± 1.2$^{(1)}$	96.1 ± 0.4
R	$H_2SO_{4(l)}$	−690.1	−814.0	156.9
P	$UO_2SO_{4(l)}$	−1714.5 ± 1.8	−1908.8 ± 2.2	46.01 ± 6.17
W	$H_2O_{(l)}$	−237.14	−285.83	69.95

Data from (Grenthe et al., 2004; Torrero et al., 1997); [1]All standard enthalpy values are at temperature $T = 25$ °C and pressure. $P = 1$ atm; the Gibbs free energy: $\Delta G = \Delta H - T\Delta S$. $^{(1)}$ CODATA reference values (Cox et al., 1984).

demands of deeper, low-grade mineralized layers in the mining industry.

The study first introduces the methods and flow transport model used to simulate the in-situ process, followed by a brief description of the reactive chemical transport model involved in the dissolution/precipitation of minerals. The implementation of the streamline approach on a parallel graphic card is then presented. A novel 1D analytical solution to the dissolution/transport equations for the ISL process is detailed. Finally, the paper presents results from a case study that compares the parallelized streamline approach with 3D simulation results.

2. Material and methods

An area of constant permeability with a uniform distribution of mineral/rock is considered and divided into hexagonal cells with injection wells (in red) located at its vertices and a pumping productive well (in blue) at its center (Fig. 1). The wells' screens are with a length of approximately eight meters long and are centered along the height of the layer. Constant pressure is imposed at the lateral boundaries of the region, together with impermeability conditions on the upper and lower boundaries. Well flow rates are imposed to be constant; the flow rate balance is maintained, i.e. the sum of flow rates on injection wells is kept equal to the flow rate of the production well.

Numerical modeling of the ISL requires finding solutions to a system of partial differential equations and generally consists of two major steps: (i) estimating the pressure p [Pa] and velocity $\boldsymbol{u}$ [m s^{-1}] fields using the Darcy's law and conservation laws (Eqs. (1)–(2)); (ii) solving the equations governing mass transfer for the chemical components and the conservation of the solute mass (Panfilov et al., 2016; Aizhulov et al., 2022; Bear, 2014; Darcy, 1856; Danaev et al., 2005; Chang et al., 2006):

$$\boldsymbol{u}\phi = -\frac{\boldsymbol{k}}{\mu}.(\nabla p + \rho_l \boldsymbol{g}) \tag{1}$$

$$\rho_l.\nabla.(\boldsymbol{u}\phi) = q \tag{2}$$

where ϕ [m^3 m^{-3}] is porosity, $\boldsymbol{k}$ [m^2] the intrinsic permeability, μ [Pa s] the dynamic viscosity, ρ_l [kg m^{-3}] the fluid density, $\boldsymbol{g} = 9.80665$ [m s^{-2}] the gravitational acceleration, ∇ [m^{-1}] the gradient operator, $\nabla.$ [m^{-1}] the divergence operator, and q [kg m^{-3} s^{-1}] the flow rate sources. The fluid density and velocity are assumed to be spatially constant, so that ρ_l can be extracted from the divergence term and the time derivative of the velocity is zero ($\partial_t(\boldsymbol{u}\phi) = 0$) in the conservation Eq. (2). Substituting Eq. (2) into (1) gives the following stationary pressure flow mass conservative equation (Panfilov et al., 2016):

$$\nabla.(\boldsymbol{u}\phi) + \nabla.\left(\frac{\boldsymbol{k}}{\mu}.(\nabla p + \rho_l \boldsymbol{g})\right) = q^* \tag{3}$$

with $q^* = q/\rho_l$ [s^{-1}] the reduced source term which is positive for injection or negative for pumping. Iterative methods are commonly used for solving the pressure and velocity fields governed by elliptic equations (Danaev et al., 2005; Chang et al., 2006). The implicit and explicit approaches for calculating the pressure include the following numerical methods: Jacobi Iteration (JI), Point Gauss-Seidel Iteration (PGSI), Line Gauss-Seidel Iteration (LGSI), and Point Successive Over-relaxation (PSO) (Press et al., 2007). The main problem with the classical numerical iterative approaches mentioned above is that they require highly time-consuming computational resources. Calculation speed on standard desktop computers can be significantly improved using high-performance computing parallel technologies like CUDA on a GPU (CUDA, 2013). The pressure distribution for a hexagonal well pattern with the above mentioned boundary conditions are shown in Fig. 2.

Several methods exist for solving ISL mass transfer problems (Penkovskij Ben Simon et al., 2014; Regnault et al., 2015; Collet et al., 2022). However, these methods largely rely on computationally expensive 3D kinetics process modeling (Collet et al., 2022). The main concept of this study is to use a streamline-based method that splits the 3D chemical kinetics problem into a set of 1D chemical kinetics calculations along the streamlines that traverse the 3D space under investigation. This approach can significantly accelerate computer time because the problem can be easily parallelized. In addition, analytical solutions can often be found for 1D mass transfer problems for the sulfuric acid ISL of uranium as demonstrated in previous studies (Kuljabekov, 2014; Panfilov et al., 2016; Golubev et al., 1978; Penkovski and Rybakova, 1989; Kancel, 2008; Alibayeva et al., 2009; Alibayeva et al., 2010).

One of the major issues in any mass transfer numerical simulations is finding the reaction rate coefficients for specific chemical components: kinetic rate constants are the key parameters in numerical modeling. These critical kinetic rate constants can only be obtained in laboratory conditions through experimental data. Literature reports several experiments and kinetic rate constants for uranyl minerals leached by sulfuric acid (Bhargava et al., 2015; Steefel et al., 2005; Faraji et al., 2020a; Kurmanseiit et al., 2022) which describe the results and interpretation of pipe-leaching experiments. The material used in this work comes from the South Tortkuduk deposit consisting of medium-fine-grained sand with a uranium content of 0.077%, with coffinite being the dominant mineral (90%). The rate constants for leaching this ore have been determined in previous laboratory studies (Kurmanseiit et al., 2022).

The acidic leaching agent being slightly denser than groundwater, gravitational effects must be accounted for in the pressure equation as it can impact the flow direction. Due to these gravitational effects, the injected fluid, being denser, tends to move downwards, while the lighter groundwater flows towards the production well. Incorporating gravitation effects into the Computational Fluid Dynamics (CFD) can significantly complicate the streamline simulation method because it requires streamlines to be recalculated at every iteration. This is a known limitation of the streamline method (Thiele, 2001; Datta-Gupta and King, 1995; Batycky et al., 1997; King and Datta-Gupta, 1998; Crane and Blunt, 1999; Oladyshkin et al., 2008; Gerritsen et al., 2009; Thiele et al., 2010; Wen et al., 2014; Alhashmi et al., 2015; Datta-Gupta and King, 2007).

3. Reactive chemical transport

Since the total mass of the elements involved in a chemical reaction is preserved (Kurmanseiit et al., 2022), it is assumed that the density of the solution remains unchanged during the ISL process. Simple chemical reactions involving reagents, solid minerals, and leached minerals can be represented as follows:

$$\nu_1 M_{(s)} + \nu_2 R_{(aq)} = \nu_3 P_{(aq)} + \nu_4 W_{(l)}; UO_{3(s)} + H_2SO_{4(aq)} = UO_2SO_{4(aq)} + H_2O_{(l)} \tag{R1}$$

where $R_{(aq)}$ is the reagent, i.e., sulfuric acid (H_2SO_4), $M_{(s)}$ is the solid mineral consisting of uranium trioxide (UO_3), $P_{(aq)}$ is the leached mineral product uranyl sulfate (UO_2SO_4) and water $W_{(l)}$ (H_2O) (Uranium Production by Country, 2022). The dissolution reaction is exothermic with a negative enthalpy, estimated to be $\Delta H = -117.0$ kJ mol^{-1} (Torrero et al., 1997) (Table 1). The liquid phase consists of three

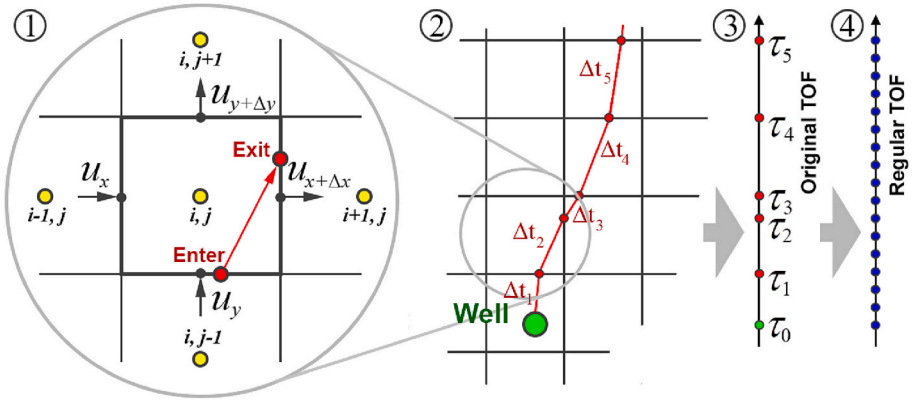

Fig. 3. 2D Schematic of regular square cells illustrating Pollock's algorithm. The streamline flow enters the cell (*i,j*) with an input velocity v_{ξ_i} which is linearly estimated throughout the cell to calculate the smallest exit time δt_m, and the exit coordinates ξ_e (see text). The streamlines are then traced from the current cell to the adjacent cell.

components: water, sulfuric acid and uranyl sulfate.

The solid phase consists of uranium trioxide and all other solid components. From reaction (R1) the mass balance equations for uranium trioxide concentration C_M, sulfuric acid concentration C_R, and uranyl sulfate concentration C_P are given by:

$$\begin{aligned} \partial_t C_M &= -\nu_1 \omega/(1-\phi) \\ \partial_t C_R + \boldsymbol{u}.\nabla C_R &= \nabla.(D\nabla C_R) - \nu_2 \omega/\phi \\ \partial_t C_P + \boldsymbol{u}.\nabla C_P &= \nabla.(D\nabla C_P) + \nu_3 \omega/\phi \end{aligned} \tag{4}$$

where C_M, C_R, and C_P are the molar concentration [mol L^{-1}] of the uranium trioxide, sulfuric acid and uranyl sulfate, respectively, t is the time [day]; ∂_t is the time derivative [day^{-1}], $\boldsymbol{u}$ is the fluid flow velocity [m day^{-1}], ν_i is the stoichiometric coefficient of component i in the chemical reaction (R1), ω is the reaction rate [mol L^{-1} day^{-1}] for the chemical reaction described by the Law of Mass Action (LMA), ϕ is the porosity, ρ_s is the molar density of the solid rocks [mol m^{-3}], and D is the dispersion coefficient [m^2 day^{-1}]. The boundary conditions are case-dependent and will be defined later in section 5 Eq. (13). In most mining applications, the diffusion terms $\nabla.(D\nabla C_i) \approx 0$, leading to a simplified set of convective Eq. (4) as follows:

$$\begin{aligned} \partial_t C_M &= -\nu_1 \omega/(1-\phi) \\ \partial_t C_R + \boldsymbol{u}.\nabla C_R &= -\nu_2 \omega/\phi \\ \partial_t C_P + \boldsymbol{u}.\nabla C_P &= \nu_3 \omega/\phi \end{aligned} \tag{5}$$

The second order reaction rate constants k [L mol^{-1} day^{-1}], which are temperature-dependent, can be expressed as (Gromov, 1978; Grenthe et al., 2004; Zheng and Wang, 1999; Kuljabekov, 2014; Panfilov et al., 2016):

$$\omega = k\, C_M C_R \tag{6}$$

The ability of acid to penetrate uraninite/coffinite inclusions in rock determines the interaction between the lixiviate and solids (Kurmanseiit et al., 2022). The reaction between liquid and solid components is a complex process and cannot always be described by a first or second-order kinetic LMA using stoichiometric coefficients from dissolution reaction (such as Guldberg-Waage or van't Hoff's law). Instead, an empirical expression with stoichiometric exponents is often used:

$$\omega = k\, C_M C_{R(aq)}^{\beta} \tag{7}$$

where β is an empirical parameter with a value between 0 and 2, $0 < \beta \leq 2$, where $\beta = 2$ for the mass action Guldberg-Waage's law. For the dissolution of uranium reaction (*R1*), β has been found to be equal to 1/3, $\beta = 1/3$, according to sources (Kuljabekov, 2014; Torrero et al., 1997). At high concentrations, the terms C_i express activities of component i, but in roll-front type uranium deposits, where uranium concentrations are typically low (about 500 mg/kg), the affinity will be approximated by the concentration.

Solving the set of differential Eqs. (3), (5) and (7) for a given geological model, mineralogical heterogeneity, and boundary conditions of an in-situ leaching (ISL) mining implementation scheme is computationally resource-intensive (Penkovskij Ben Simon et al., 2014; Regnault et al., 2015; Collet et al., 2022; Kurmanseiit et al., 2022). However, high-performance computational methods can improve numerical performance, such as implementing parallelization and using GPUs. One possible method is the streamline approach, which simplifies the problem by transforming a 3D problem into a set of one-dimensional equations to be solved along streamlines. In this study, we used a simplified chemical kinetic model of uranium dissolution to solve the equations.

4. Streamline approach and implementation

Streamlines are paths followed by particles in a three-dimensional flow and are useful in understanding fluid motion in continuous mechanics, oil and gas reservoir modeling, and reactive transport. The widely accepted Stream-Based Flow Modeling approach is effective in capturing the physics of flow displacement with an approximate 1D model along each streamline. Over the past two decades, much attention has been given to streamline-based flow modeling, leading to the widely accepted Stream-Based Flow Modeling (SFM) approach as an effective and complementary technology to classical flow simulation methods such as finite volume and finite differences (Thiele, 2001). Streamlines are intensively used (Thiele, 2001; Datta-Gupta and King, 1995; Batycky et al., 1997; King and Datta-Gupta, 1998; Crane and Blunt, 1999; Oladyshkin et al., 2008; Gerritsen et al., 2009; Thiele et al., 2010; Wen et al., 2014; Alhashmi et al., 2015; Datta-Gupta and King, 2007). The advantage of the streamline-based method is its ability to use a dimensionless variable change to express the transport equation as a function of the time of flight (TOF) along the streamline trajectory. This approach captures the physics of the flow displacement with an approximate 1D model along each streamline (Peng et al., 2009).

The Pollock's tracing method (Pollock, 1988) is a popular algorithm for tracing streamlines of a velocity field given at the nodes of a 3D Cartesian cell mesh. The method can be implemented in three steps: (i) resolving the pressure equation for calculating the velocity field; (ii) tracing the streamline trajectories from the velocity field; and (iii) resolving the 1D reactive transport equation along the streamlines. Pollock's algorithm involves calculating the total flux entering and exiting each cell using Darcy's Law, solving transport equations along streamlines using time-of-flight (TOF) instead of spatial coordinates, and determining the streamline exit point and exit time given any entry point in each coordinate direction. Assuming a piecewise linear

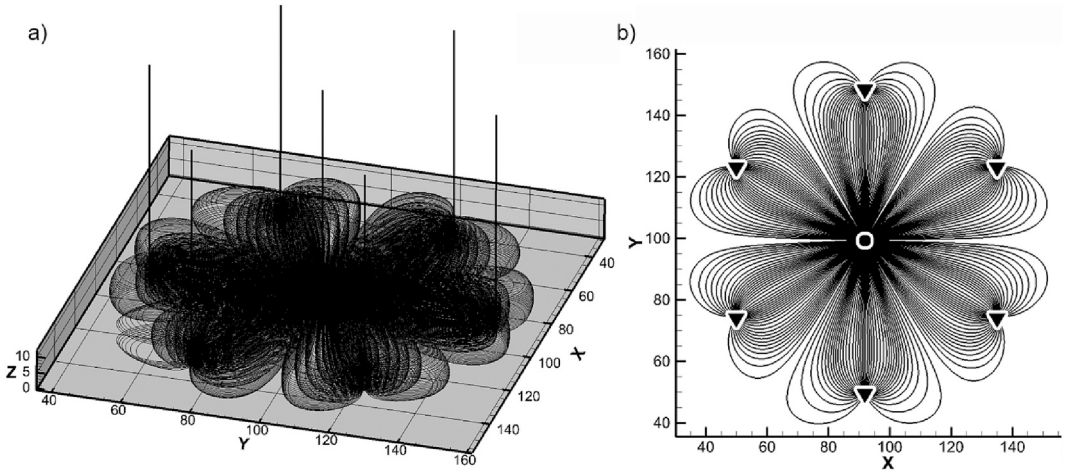

Fig. 4. Paths of streamlines are traced in (a) 3D space and (b) top view using Pollock's algorithm for a hexagonal injection pattern with a production well located at the center.

approximation of the interstitial velocity field $v = u/\phi$ [m s^{-1}] within cells, the following simple formulation can be derived for the velocity at any location (Thiele, 2001):

$$v_x = v_{x_0} + g_x(x - x_0) = dx/dt; g_x = \left(v_{x_{\delta x}} - v_{x_0}\right)/\Delta x \tag{8}$$

where v_{x_0} is the velocity component along the x-axis of the grid at $x = x_0$, and g_x is the velocity gradient in the x-direction. Similar expressions are obtained for the y- and z- directions. To write synthetic formulas valid for any direction, let $\xi \in \{x, y, z\}$ be the x-, y- or z- coordinate. Given an arbitrary entry point $(\xi_i \in (x_i, y_i, z_i))$ (Fig. 3), the exit-times out of each face are obtained by integrating velocities $v_{\xi_i}, \xi_i \in \{x_i, y_i, z_i\}$ according to:

$$\delta t_\xi = \frac{1}{g_\xi} ln\left[\frac{v_{\xi_0} + g_\xi(\xi_e - \xi_0)}{v_{\xi_0} + g_\xi(\xi_i - \xi_0)}\right] \xi \in \{x, y, z\} \tag{9}$$

where $\xi_e = (x_e, y_e, z_e)$ represents the unknown exit coordinates. The streamline exits the cell from the face having the smallest exit time $\delta t_m = \min_{\xi \in \{x,y,z\}} (\delta t_\xi)$. After that, the exit locations can be determined by solving Eq. (9) for $\xi_e \in (x_e, y_e, z_e)$ using the minimum time δt_m:

$$\xi_e = \frac{1}{g_\xi} ln\left[v_{\xi_i} exp\left(g_\xi \delta t_m\right) - v_{\xi_0}\right] + \xi_0; \xi \in \{x, y, z\} \tag{10}$$

Pollock's formulation is originally derived for an orthogonal grid block. However, an isoparametric transformation (Cordes and Kinzelbach, 1994) can be employed to convert a corner-point geometry grid into unit cubes or curvilinear coordinates (Prévost et al., 2001) for use on any unstructured grid commonly utilized in reservoir simulation. Fig. 3 illustrates this approach, where the differential equations remain the same for each streamline, differing only by their initial and boundary conditions (i.e., input and exit velocities). One of the advantages of Pollock's algorithm is that it does not require the resolution of differential equations for each cell since each 1D domain has its specific length and initial and boundary conditions. Fig. 4 shows the streamline paths traced in (a) 3D space and (b) top view, calculated using Pollock's algorithm for a hexagonal injection schema with a production well at the center. To display streamlines more effectively, the visualization domain is reduced to a section of the block from 30 m to 160 m in the x direction and from 35 m to 165 m in the y direction (Fig. 4; Fig. 7a; Fig. 9).

5. 1D analytical solution to the reaction transport equation

The pressure equation, including the gravity term, is solved using a classical finite differences method on a regular grid in the three-dimensional space with given boundary conditions and injection/production rates. The resulting velocity field is used to calculate streamlines or stream tubes using Pollock's algorithm for solving the kinetic eq. A local parametric system attached to each streamline simplifies the problem into a 1D transport problem with reactive transport terms. This approximation of the full 3D problem neglects radial diffusive terms and only a 1D solution is required to evaluate the in-situ leaching (ISL) process. The Eq. (5) is rewritten in terms of concentrations (C_i) and time-of-flight (TOF) along the streamline. The convective spatial derivative with respect to the curvilinear coordinate is defined as the partial derivative against the TOF ($\partial_\tau = u\,\partial_s$), and the TOF is the time necessary for a single particle to travel from the origin of the streamline to a curvilinear coordinate (s) under the influence of the flow velocity field (u). The resulting equation is as follows:

$$\begin{aligned} (1-\phi)\partial_t C_M + \nu_1 \omega &= 0 \\ \phi\,(\partial_t C_R + u\,\partial_x C_R) + \nu_2 \omega &= 0 \\ \phi\,(\partial_t C_P + u\,\partial_x C_P) - \nu_3 \omega &= 0 \\ \omega = k\,C_M\,C_R^\beta \end{aligned} \tag{11}$$

where indices 1, 2 and 3 represent M, R, and P, respectively. The TOF $\tau(s)$ along the streamline at the curvilinear dimensionless coordinate ($s = x/l, s \in [0, 1]$) is defined as $\tau(s) = \int_0^s d\zeta/u(\zeta)$, with x the curvilinear distance along the streamline and l is the total length. This provides a measure of the time taken for a single particle entering the streamline at $t = 0$ to travel to a point along the streamline defined by the curvilinear coordinate s under the influence of the flow velocity field $\boldsymbol{u}$. Introducing the two parameters (if porosity varies, it is spatial-dependent quantity) $\lambda_1 = \nu_1 k/(1-\phi)$ and $\lambda_2 = -\lambda_3 = \nu_2 k/\phi$, Eqs. (11) can be simplified into (reminding $\nu_1 = 1$):

$$\begin{aligned} \partial_t C_M + \lambda_1 C_M C_R^\beta &= 0 \\ \partial_t C_R + \partial_\tau C_R + \lambda_2 C_M C_R^\beta &= 0 \\ \partial_t C_P + \partial_\tau C_P - \lambda_3 C_M C_P^\beta &= 0 \end{aligned} \tag{12}$$

The initial and boundary conditions are:

$$C_M|_{t=0} = C_M^0(\tau); C_R|_{t=0,\tau\geq 0} = 0; C_R|_{t>0,\tau=0} = C_R^{inj}; C_P|_{t=0} = 0; C_P|_{\tau=0} = 0 \tag{13}$$

These initial conditions mean that: (i) at initial time $t = 0$, the uranium concentration along the streamline is equal to $C_M^0(\tau) = C_M(\tau, 0)$; (ii) a constant concentration in acid C_R is continuously injected at $t > 0$, and that the system is not productive at the initial time $t = 0$.

5.1. 1D asymptotic solution to the hyperbolic system

Given arbitrary initial data, an asymptotic analytical solution to the hyperbolic Eqs. (12) can be derived. The concentrations of acid and water, C_R, are generally much higher than the initial molar concentrations of ore and liquid, C_M and C_P. As such, they are assumed to be of the order $\varepsilon = C_M^0$, where $0 < \varepsilon \ll 1$. A series approximation to the second order in ε is used to provide a solution to the system as follows (Kuljabekov, 2014; Panfilov et al., 2016):

$$C_M = \varepsilon + O(\varepsilon^2); C_R = C_R^0 + \varepsilon\, C_R^1 + O(\varepsilon^2); C_P = C_P^0 + \varepsilon\, C_P^1 + O(\varepsilon^2) \tag{14}$$

The zero-terms C_i^0, where $i \in \{R, P\}$, satisfy a shock wave-type equation similar to saturation or Buckley-Leverett equations. The boundary conditions are defined by Eq. (13). The exact solution of a hyperbolic equation has a simple form in which the concentration of acid in water, $C_R^0(\tau, t) = C_R^0(t - \tau)$, depends only on the difference between the current time, t, and the time of flight along the streamline, τ. For a specific case, the solution is a step shock wave, which can be expressed using the Heaviside function, $H(s)$, as follows (Kuljabekov, 2014; Panfilov et al., 2016):

$$C_R^0(\tau, t) = C_R^{inj} H(t - \tau); H(s) = \begin{cases} 1; s > 0 \\ 0; s \le 0 \end{cases} \tag{15}$$

In a coordinate system attached to the streamline, the dynamic front wave $\tau(s) = t$ represents the propagation of the injected-solution front. When the TOF τ is greater than the current time t ($\tau > t$), the concentration of acid in water is zero $C_R^0(\tau > t, t) = 0$, and it reaches its maximum value when $\tau = t$, at which point the uranium ore starts to dissolve. To solve the linear terms $C_i^1, i \in \{R, P\}$, we substitute Eqs. (14)–(15) into Eq. (12) which leads to the following linear system:

$$\begin{aligned} &\partial_t C_R^1 + \partial_\tau C_R^1 + \lambda_2 C_M \left(C_R^{inj}\right)^\beta H(t - \tau) = 0; C_R^1\big|_{t=0,\tau\ge 0} = 0 \\ &\partial_t C_P^1 + \partial_\tau C_P^1 - \lambda_2 C_M \left(C_R^{inj}\right)^\beta H(t - \tau) = 0; C_P^1\big|_{t=0,\tau\ge 0} = 0 \end{aligned} \tag{16}$$

where λ_2 is a constant, and C_M is the molarity of the solution. The equations describe the concentration of reactants in the system as a function of time and TOF along the streamline. Assuming a constant porosity along the streamline path, so that no clogging occurs during the leaching process (i.e. λ_1 and λ_2 are spatially and time-independent), the solutions to Eq. (16) are the exponentials given by (Kuljabekov, 2014):

$$\begin{aligned} C_R^1(\tau, t) &= -\tau\, \lambda_2 C_M^0 \left(C_R^{inj}\right)^\beta e^{-\lambda_1 \left(C_R^{inj}\right)^\beta (t-\tau)} H(t - \tau) \\ C_P^1(\tau, t) &= -C_R^1(\tau, t) = \tau\, \lambda_2 C_M^0 \left(C_R^{inj}\right)^\beta e^{-\lambda_1 \left(C_R^{inj}\right)^\beta (t-\tau)} H(t - \tau) \end{aligned} \tag{17}$$

The solutions are expressed as a function of the molar concentration of acid, $C_R(\tau, t)$. The time-evolution of the uraninite concentration, $C_M(\tau, t)$, at the location τ in the ore depends on the total amount of acid, $C_R(\tau, t)$, which has percolated through the ore, as given by:

$$C_M(\tau, t) = C_M^0(\tau)\, e^{-H(t-\tau) \int_0^t \lambda_1 \left(C_R^{inj}(\tau,\zeta)\right)^\beta d\zeta} \tag{18}$$

By using the first-order approximation term of the reagent concentration C_R^{inj} from Eq. (15) and assuming that the coefficient λ_1 is stationary (i.e. porosity does not evolve through time, making λ_1 time-independent), Eq. (18) can be simplified into a more classical form, as shown in (Kuljabekov, 2014; Panfilov et al., 2016):

$$C_M(\tau, t) = C_M^0(\tau)\, e^{-\lambda_1 \left(C_R^{inj}\right)^\beta (t-\tau) H(t-\tau)} = C_M^0(\tau) \left\{ 1 - \left(1 - e^{-\lambda_1 \left(C_R^{inj}\right)^\beta (t-\tau)} \right) H(t - \tau) \right\} \tag{19}$$

Under the above approximations, the final one-dimensional analytical solutions for a leaching process occurring along any streamline can be derived. These solutions are summarized in Eq. (20).

Final 1D solution: Assuming a constant rate of acid injection, the 1D analytical solution for the set of differential Eq. (12) yields a shock wave followed by a decreasing exponential function. The final solution can be expressed as follows:

$$\begin{aligned} C_M(\tau, t) &= C_M(\tau, 0) \left\{ 1 - \left(1 - e^{-\lambda_1 \left(C_R^{inj}\right)^\beta (t-\tau)} \right) H(t - \tau) \right\} \\ C_R(\tau, t) &= \left\{ C_R^{inj} - \tau\, \lambda_2 C_M(\tau, 0) \left(C_R^{inj}\right)^\beta e^{-\lambda_1 \left(C_R^{inj}\right)^\beta (t-\tau)} \right\} H(t - \tau) \\ C_P(\tau, t) &= \tau\, \lambda_2 C_M(\tau, 0) \left(C_R^{inj}\right)^\beta e^{-\lambda_1 \left(C_R^{inj}\right)^\beta (t-\tau)} H(t - \tau) \\ \lambda_1 &= \frac{\nu_1 k}{(1 - \phi)}; \lambda_2 = \frac{\nu_2 k}{\phi}; \lambda_2 = -\frac{\nu_3 k}{\phi}; \tau(x) = \int_o^{x/l} \frac{d\zeta}{u(\zeta)}; \tau \ge 0 \end{aligned} \tag{20}$$

where $\tau(x)$ the time of flight (TOF) counted from the origin to reach a location x along the streamline of length l [m], x is the curvilinear distance [m] along the streamline counted from its origin, and u is the fluid particle velocity [m s^{-1}] percolating the porous media of porosity ϕ. All quantities are expressed in SI units. The molar concentration of uranium in the ore at time t [day] and location τ (expressed in TOF) [day] is denoted by $C_M(\tau, t)$ [mol L^{-1}]. $\lambda_i, (i = 1, 2, 3)$ is the (modified) rate constant [L mol^{-1} day^{-1}], and $\nu_i, (i = 1, 2, 3)$ is the stoichiometric coefficient for species i involved in the chemical dissolution reactions. The term $C_R^{inj} = C_R(0, t)$ represenets the amount [mol L^{-1}] of acid injected at a constant rate in the system; β is an empirical parameter (equal to $\beta \approx 1/3$ for uranium (Torrero et al., 1997)). The Heaviside function is denoted by H; $C_M(\tau, t)$ is the molar concentration [mol L^{-1}] of reagent at (t, τ); and $C_P(\tau, t)$ is the molar concentration [mol L^{-1}] of uranyl sulfate (product).

5.2. Ore recovery

Each streamline drains a cross-sectional area $S(\tau)$ in the three-dimensional ore deposit corresponding to a total amount of in-situ uranium-trioxide $q_M(0) = q_{UO_3}(0)$ at time $t = 0$ (i.e. before the leaching starts) given by:

$$q_M(0) = \int_0^1 (1 - \phi(\tau))\, S(\tau)\, C_M(\tau, 0)\, d\tau = (1 - \phi)\, S \int_0^1 C_M(\tau, 0) d\tau \tag{21}$$

The total cumulative amount of in-situ recoverable uranium $q_M(t)$ produced by a streamline at time t is given by integrating the concentration $C_P(1, t)$ over time; it becomes:

$$q_P(t) = \int_0^t \phi(\tau)\, S(\tau)\, C_P(1, \xi)\, d\xi = \phi\, S \int_0^t C_P(1, \xi) d\xi \tag{22}$$

The simplified second members of Eqs. (21) and (22) are valid when the porosity and the section S are constant all along the streamlines. The recovery $R(t)$ defined in the range [0,1] is the ratio of the cumulative uranium $q_P(t)$ leached at the time t and dissolved as a product P in the liquid, to the potential in place recoverable uranium $q_M(0)$:

$$R(t) = \frac{q_P(t)}{q_M(0)} = \frac{\int_0^t \phi(\tau)\, S(\tau)\, C_P(1, \xi)\, d\xi}{\int_0^1 (1 - \phi(\tau))\, S(\tau)\, C_M(\tau, 0)\, d\tau} = \frac{\phi}{(1 - \phi)} \cdot \frac{\int_0^t C_P(1, \xi) d\xi}{\int_0^1 C_M(\tau, 0) d\tau} \tag{23}$$

Inserting Eq. (20) in Eq. (23) shows that the recovery $R(t)$ is a cumulative exponential distribution given by:

$$R(t) = \left\{ 1 - e^{-\frac{k C_R^{inj} (t-\tau)}{(1-\phi)}} \right\} H(t - \tau) \tag{24}$$

assuming $\beta = 1$, if not the followings are valid substituting C_R^{inj} by $\left(C_R^{inj}\right)^\beta$, where τ is the time necessary to reach the producer from the injector wells when the injection starts at $t = 0$. Notice that for an infinite time, the recovery is equal to 1 ($R(t \to \infty) = 1$). The recovery rate $\partial_t ln(1 - R) = -\partial_t R/(1 - R)$ is defined as the log-derivative with respect

Table 2
Ore and solution characteristics used to numerically solve the reactive transport system described by Eq. (20).

ϕ	ρ_s	ρ_l	K_f	y_M	$(H_2SO_{4(liquid)})$
[%]	[kg m^{-3}]	[kg m^{-3}]	[m day^{-1}]	[%]	[g L^{-1}]
0.22	1700	1015	7.0	0.077	20

to time t of one minus the recovery $1 - R(t)$. The constant α is proportional to the injected amount of sulfuric acid $C_R^{inj} = C_{H_2SO_4}^{inj} = C_R(0,t)$, the chemical (temperature and pressure-dependent) rate constant k, and inversely proportional to the porosity (rock density1700 [kg m^{-3}]):

$$\partial_t ln(1-R) = -\frac{\partial_t R}{1-R} = -\frac{kC_R^{inj}}{(1-\phi)} = \alpha$$
$$ln(1-R(t)) = \alpha(t-\tau)H(t-\tau) = \frac{(t-\tau)}{\tau_{SCM}} H(t-\tau) \tag{25}$$

A log-time plot of the quantity $1 - R(t)$ against time t shows a horizontal line at 0 up to time τ, followed by a decreasing line with a constant negative slope of $\alpha = 1/\tau_{SCM}$ [day^{-1}]. By knowing the porosity ϕ and the constant amount of injected acid C_R^{inj}, the rate constant k can be estimated graphically as $k = |\alpha|(1-\phi)/C_R^{inj}$. This analytical model can be used to test the numerical resolution of the set of Eq. (12). The quantity τ_{SCM} is the time constant [day] in the liquid film diffusion control, which is the completion time required for the diffusion process in the layer formed at the surface of the particles. According to (Li et al., 2013; Faraji et al., 2020b), the time constant τ_{SCM} is defined as:

$$\tau_{SCM} = \frac{\rho_M R_0}{\nu_1 k_c C_R^{inj}} \tag{26}$$

The expression (26) shows that τ_{SCM} is proportional to the molar density [mol m^{-3}] of the reactive component in the solid ρ_M, and to the initial radius of the solid particle, R_0 [m]. It is also inversely proportional to the mass transfer coefficient in the liquid film k_c [m day^{-1}], to the stoichiometric coefficient of the reactant, ν_1, and to the molar concentration of leaching agent, C_R^{inj} (mol m^{-3}).

Eq. (25) represents a log-time-linear recovery equation that is commonly used to describe leaching kinetic model in the shrinking core model (SCM), which is a first-order leaching kinetic model. The SCM is a widely used model for describing the dissolution kinetics (Li et al., 2013; Faraji et al., 2020b) in leaching processes of minerals. The model

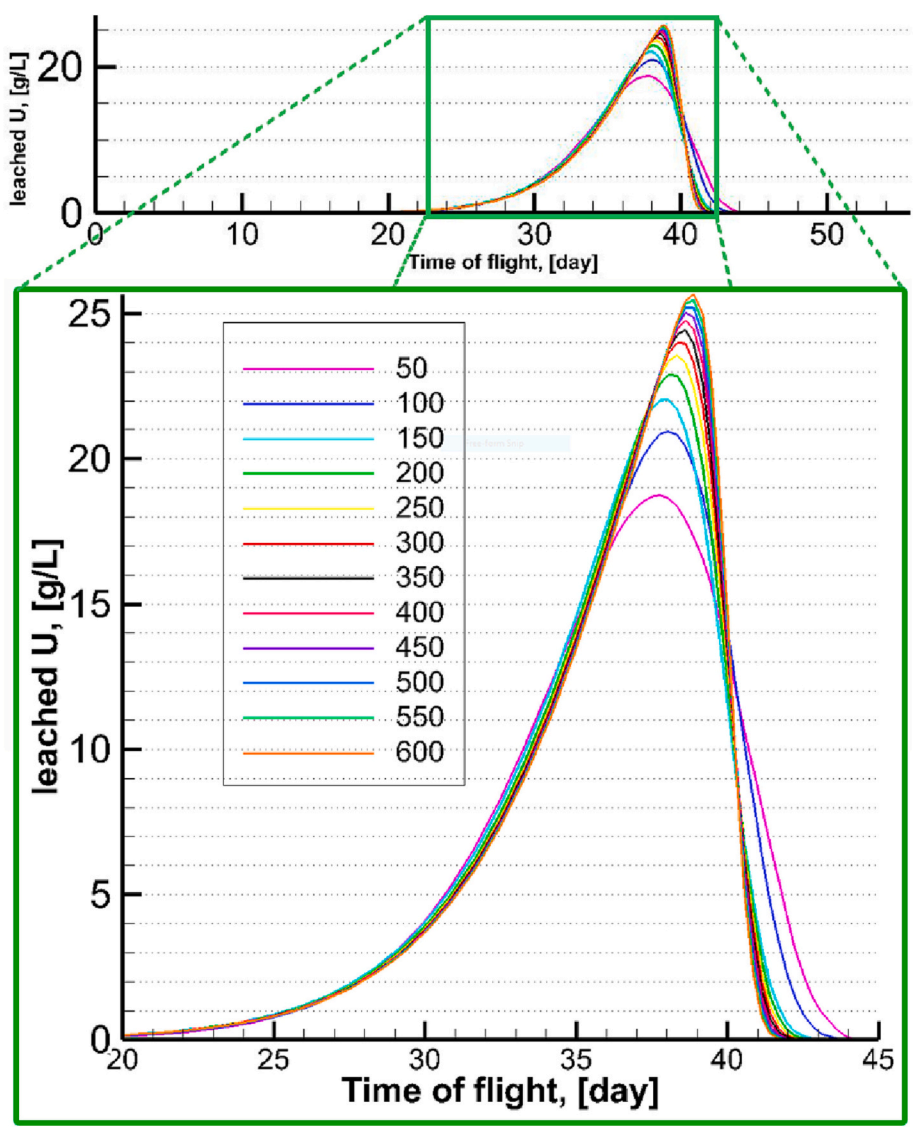

Fig. 5. Leached uranium (U) distribution [in g L^{-1}] along the streamlines for different mesh sizes ranging from 50 to 600 nodes. The 500-nodes mesh provides an acceptable level of precision for determining the acid concentration.

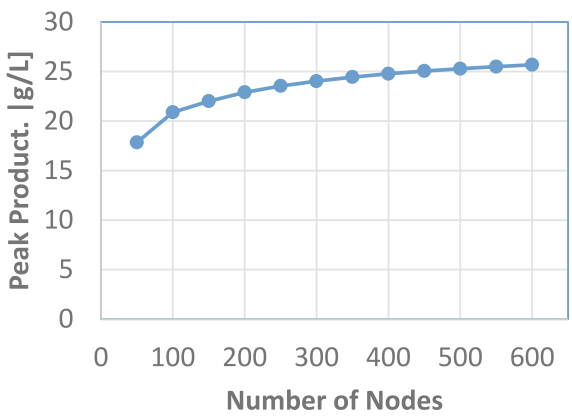

Fig. 6. Variation of peak value of leached mineral [g L^{-1}] along streamlines for different mesh sizes ranging from 50 to 600 nodes. The plot shows that the peak value stabilizes and converges for a mesh size of 500 nodes, which is then used for further numerical experiments.

involves several mechanisms including liquid film diffusion control, chemical reaction control at the grain surface, and solid product layer diffusion control. The slowest process among these mechanisms determines the final leaching kinetics. The SCM assumes that leaching rate is proportional to both the concentration of the leaching agent and the surface area of the mineral, based on the radius as well as the porosity of the particle. This first-order leaching kinetic model can be used to predict the leaching behavior of minerals under various conditions, such as temperature, concentration, and particle size. In the present case, the log-time-linear recovery expression indicates that liquid film diffusion control is the dominant process, and that the size of the solid particle remains approximately constant (Faraji et al., 2020b).

In the context of reserve estimation, the mass percentage is commonly employed as the unit of measure for uranium content. Nevertheless, when engaging in mathematical modeling, it becomes essential to work with moles in accordance with the law of conservation of mass. However, engineers typically find values expressed in grams per liter [g L^{-1}] more familiar. Therefore, the calculation results were converted to the appropriate units of measurement for calculation purposes and ease of comprehension by engineers. Unit conversion from mass percentage to molar concentration is done through the following formula:

$$C = \frac{\rho\, y}{M} \tag{27}$$

where C is molar concentration, ρ is density of liquids or solids depending on the component state, y is concentration in percent, M is molar mass of respective component. Therefore, as per Table 2 molar concentrations per liter of uranium and reagent are equal to:

Table 4
Comparison of the analytical and numerical results along a streamline.

	Concentrations of		
	Uranium in ore U	Sulfuric acid H_2SO_4	Leached uranium U
NRMSD, [%]	7.35	4.23	7.31
RMSD, [g L^{-1}]	0.0962	0.8463	3.4723
MAE, [g L^{-1}]	0.0465	0.3221	1.0305

RMSD = root-mean-square deviation; NRMSD = normalized root-mean-square deviation; MAE = mean absolute error.

Table 3
Peak value and relative difference of uranium concentration in the pregnant solution for different mesh sizes along the streamline.

Nodes number	50	100	150	200	250	300	350	400	450	500	550	600
$max\ (C_{leached\ U})$ [g L^{-1}]	17.9	20.9	22.0	22.9	23.5	24.0	24.4	24.8	25.0	25.3	25.5	25.7
Relative Difference [%]	30.5	18.7	14.3	10.8	8.3	6.4	4.9	3.5	2.5	1.6	0.8	–

The 500-nodes mesh provides an acceptable level of accuracy.

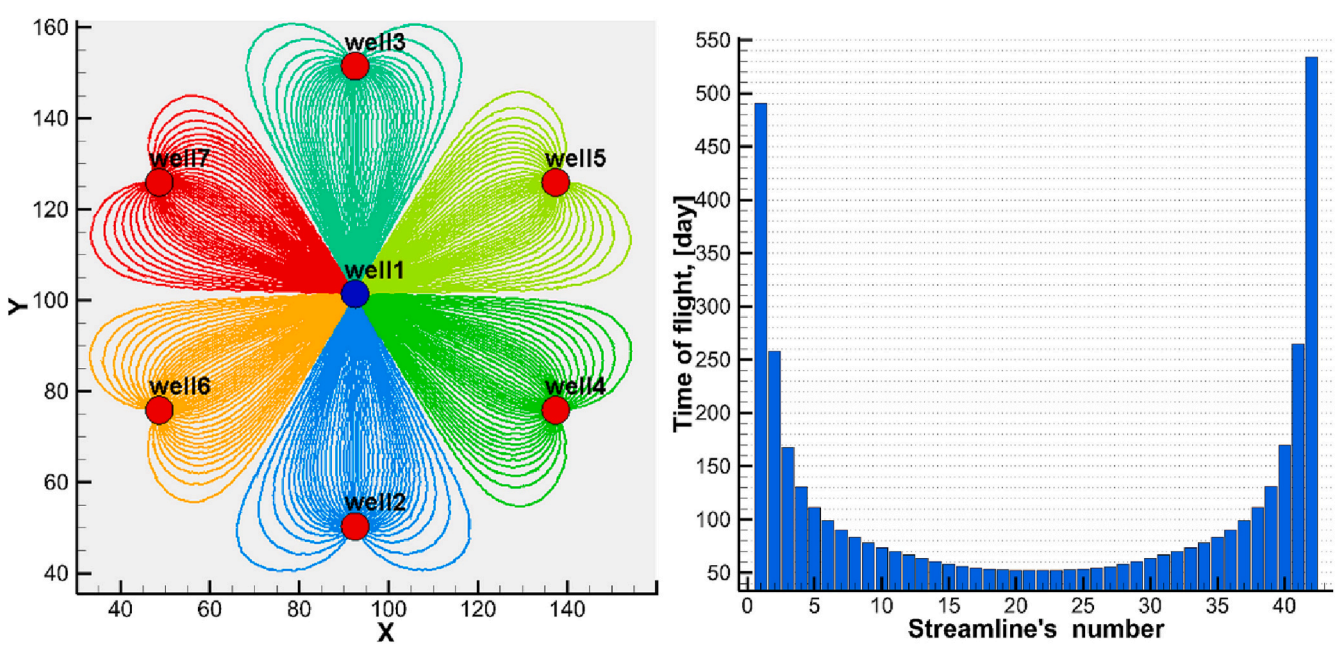

Fig. 7. (a) Top view of streamlines colored by injectors, from the injection wells to the production well. (b) Times of flight (TOF) for all streamlines from injector 2 to productor 1.

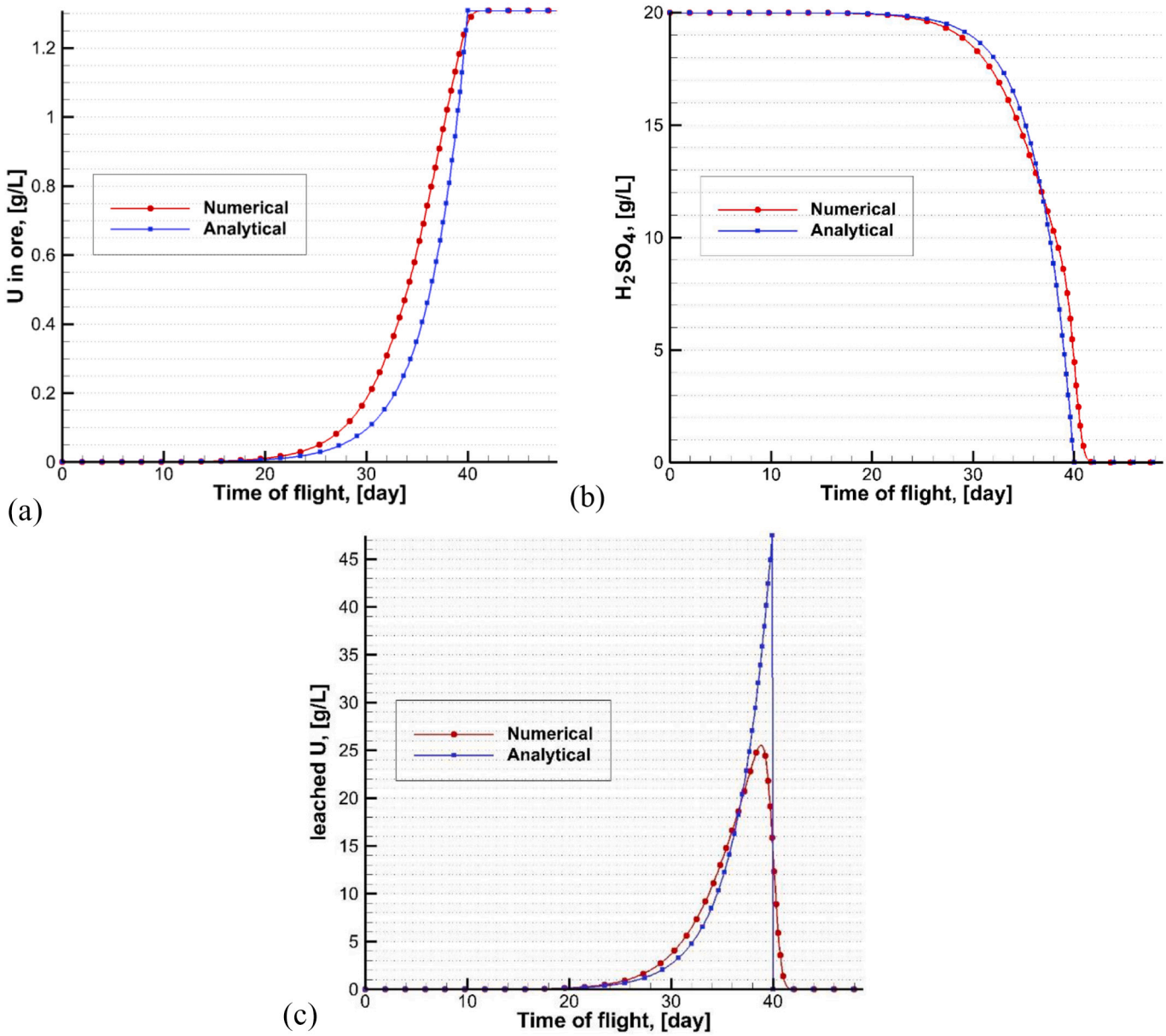

Fig. 8. Comparison of the analytical (red circles) to the numerical (blue squares) concentrations (g L^{-1}) of uranium in ore (a), sulfuric acid (b), and leached uranium (c) distributions along the shortest streamline after 40 days of mining. (For interpretation of the references to colour in this figure legend, the reader is referred to the web version of this article.)

$C_M^0 = 1.309\ [\text{mol L}^{-1}] = 1.301\ [g\ \text{L}^{-1}], C_R^{inj} = 0.2108\ [\text{mol L}^{-1}]$

6. Results

To validate the assumptions made in the analytical approximative solution of the system of Eqs. (20) and (25), we performed a numerical resolution of the same system using the initial data presented in Table 2. We calculated the distributions of solid mineral UO_3, reagent H_2SO_4, and dissolved useful components UO_2SO_4 along the streamline both numerically and analytically by solving the differential Eq. (12) on a 1D regular mesh. Based on the calculated values of the concentrations of the solid mineral UO_3 and the dissolved useful component UO_2SO_4, the concentrations of uranium in ore and leached uranium are determined and presented at all subsequent figures. To study numerical convergence and precision, we investigated several mesh sizes ranging from 50 to 600 nodes to calculate the concentrations along the streamlines (Fig. 5). The concentration of leached mineral U [g L^{-1}] is a useful indicator of the product concentration in the reagent. We calculated this concentration for different mesh sizes ranging from 50 to 600 nodes spread along the streamlines. The concentration curves stabilized and converged for a mesh size of 500 nodes, which we used for further numerical experiments (Fig. 6).

The maximum dissolved product concentration occurs at time-of-flight (TOF) between 20 and 45 days and remains constant for other values outside this range. Therefore, we focused on this specific TOF range in our analysis. We compared the peak of dissolved uranium concentration in the pregnant solution for different node numbers along the streamline (Table 3). The comparative analysis showed that the relative difference (calculated from the 600 nodes) at 500 nodes was insignificant and did not exceed 2%. Therefore, we used 500 nodes along streamlines for further calculations.

Fig. 7a presents the streamlines colored by injectors that run from the injection wells to the production well. The TOF of the streamlines from injector 2 to productor 1 are shown in Fig. 7b. The solution injected at

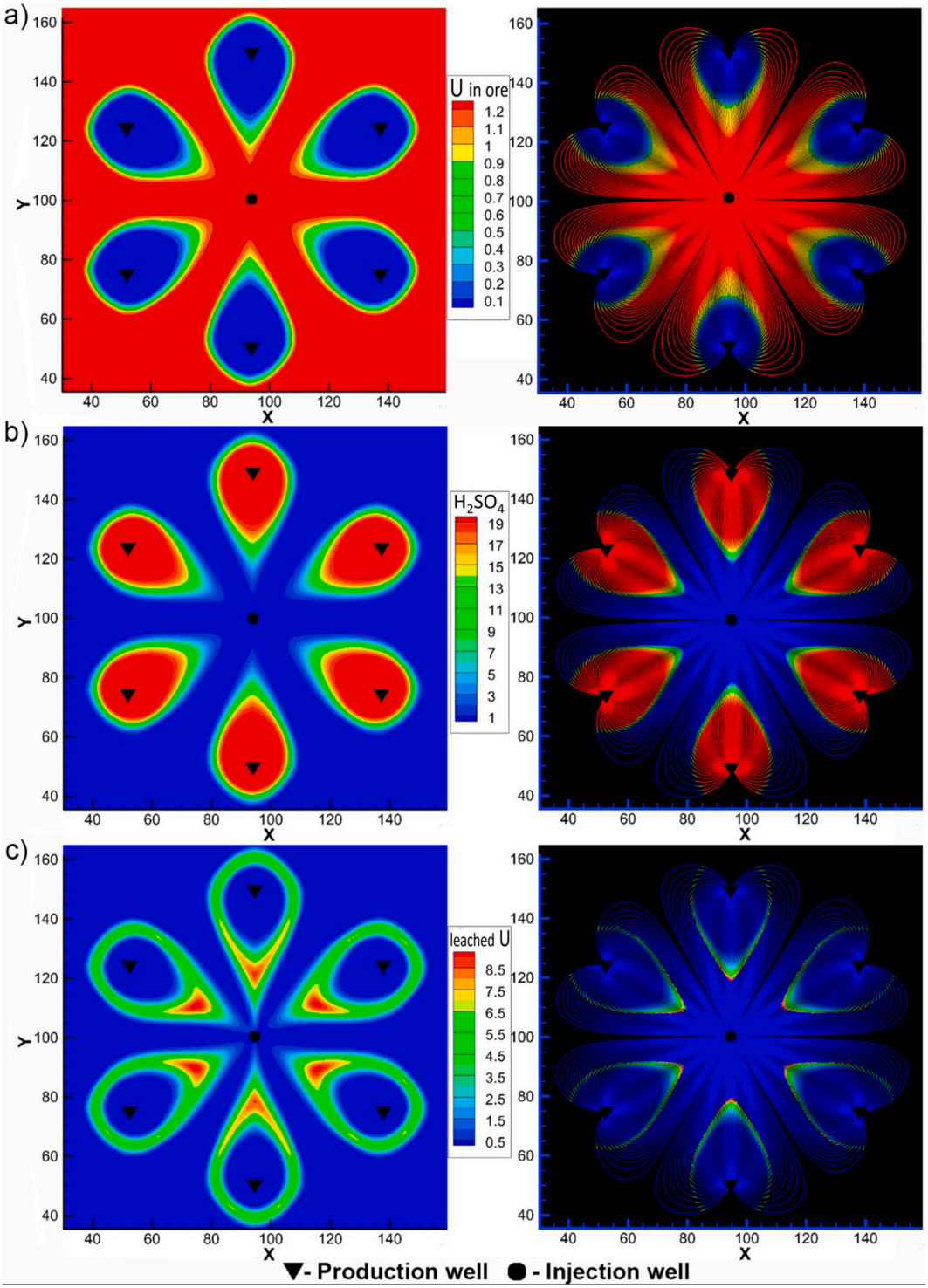

Fig. 9. Top-down view of a hexagonal well pattern (X and Y refers to Figs. 1 and 2), showing the concentration distribution (g L^{-1}) of uranium in ore (a), sulfuric acid (b), and leached uranium (c) after 40 days of ISL. Results are from 3D simulations (1st column) and streamline (2nd column) simulations.

well 2 takes 52 days to reach well 1 along the shortest streamlines. A comparative analysis of acid consumption, solid, and dissolved minerals in the ore was performed for analytical and numerical solutions along the streamline, as shown in Table 4. The relative difference in the total uranium in ore, defined as the sum of solid and dissolved uranium, between the analytical and numerical calculations was found to be <8%.

The concentrations of the uranium in ore (a), sulfuric acid (b), and leached uranium (c) are calculated along the streamlines after the 40th day of mining (Fig. 8), following the injection hexagonal pattern described in Fig. 1. The results demonstrate good agreement between the analytical and numerical solutions, with insignificant numerical diffusion observed in zones dominated by the concentration gradient. The results are qualitatively similar and in general, show good agreement (Table 4).

Fig. 9 presents top views of a hexagonal well pattern painted with concentration (g L^{-1}) of uranium in ore, (a), sulfuric acid (b), and leached uranium (c) simulated using 3D (1st column) and SL (2nd column) numerical methods after 40 days of ISL. The results are shown in

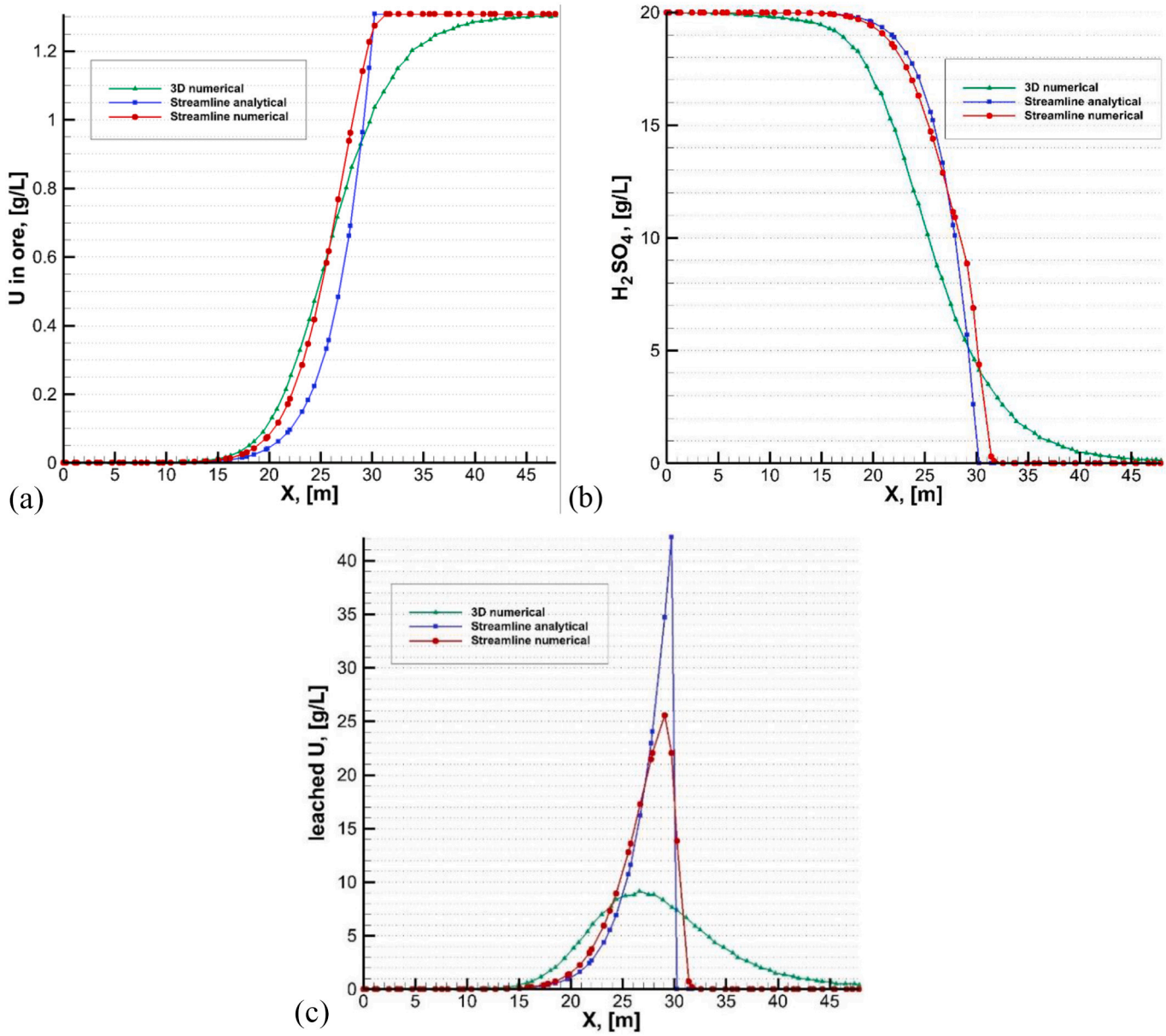

Fig. 10. Analytical (blue squares), numerical (red circles), and 3D simulation (green triangles) of (a) uranium in ore, (b) sulfuric acid, and (c) leached uranium distributions along the streamline after 40 days of ISL. The 1D analytical solution is rather close to the 1D numerical solution along the streamlines, while the full 3D numerical solution presents a wider numerical dispersion indicating lower production yield. (For interpretation of the references to colour in this figure legend, the reader is referred to the web version of this article.)

Table 5
Analytical and numerical results along streamline compared to the 3D numerical resolution.

	Concentration of					
	uranium in ore U		sulfuric acid H_2SO_4		leached uranium U	
	3D numerical	3D numerical	3D numerical	Streamline Numerical	3D numerical	Streamline Numerical
NRMSD, [%]	8.03	8.03	11.26	4.45	14.12	7.78
RMSD, [g L^{-1}]	0.1052	0.1052	2.2520	0.8909	5.9596	3.2828
MAE, [g L^{-1}]	0.0635	0.0635	1.4420	0.2976	2.7974	0.9416

RMSD = root-mean-square deviation; NRMSD = normalized root-mean-square deviation; MAE = mean absolute error.

the area between x and y intervals of [30, 160] and [35, 165], respectively, as mentioned earlier. Fig. 10 compares the concentrations of the uranium in ore (a), sulfuric acid (b), and leached uranium (c) calculated along the shortest streamline after 40 days of ISL using the analytical (blue), numerical (red), and 3D (green) simulations. The shortest streamline between the injection and production wells is about 50 m long. The analytical and numerical streamline solutions are in good agreement with a small deviation ranging from 22 to 33 m, while the 3D modeling results differ in the range of 15 to 45 m. Table 5 shows the deviation of the values of concentrations of uranium in ore, sulfuric acid,

Table 6
Computational time required to simulate in-situ leaching on a hexagonal well pattern using streamline and 3D simulations with analytical and various numerical methods.

Grid size[1]	Simulation	Method	Computation time, [s]	Ratio
		Analytical	2.74	–
	Streamline	Numerical	23.89	9
		Explicit	1208	440
$93 \times 100 \times 40$, $\Delta x = \Delta y = 2$, $\Delta z = 0.3$	3D	Explicit with multicore parallelization	190	69
		Analytical	7.78	–
	Streamline	Numerical	27.54	3.5
		Explicit	12,122	1560
$186 \times 200 \times 40$, $\Delta x = \Delta y = 1$, $\Delta z = 0.3$	3D	Explicit with multicore parallelization	2106	270

[1] Computational time is given for an Intel core i9-9900K, 3.6 GHz, RAM: 32 GB. The simulations were conducted for two different mesh sizes: $93 \times 100 \times 40$ and $186 \times 200 \times 40$.

and leached uranium obtained numerically in 3D and along the streamline with an analytical solution.

(a) (b) (c)

(a) (b)

(c)

The 3D modeling exhibits an exceedingly large numerical dispersion effect due to the 3D mesh size. To reduce numerical dispersion and computation time, several numerical methods were investigated with two mesh sizes: $\Delta x = \Delta y = 2$ m, $\Delta z = 0.3$ m and $\Delta x = \Delta y = 1$ m, $\Delta z = 0.3$ m. The 3D simulations were conducted using implicit and explicit methods; they have not given any noticeable difference in reducing numerical diffusion effects.

The numerical solution along streamlines takes 3.5–9 times longer to compute than the analytical solution, depending on the mesh size. Nevertheless, numerical solutions along streamline are significantly faster than 3D solutions, which require 70 and 440 times more computation time for multicore parallelization and simple-core explicit methods, respectively. Increasing the mesh size by a factor of four, leads to a 5.5 to 6 times increase of computational time (Table 6).

7. Conclusions

In the context of uranium mining using in-situ leaching (ISL) methods, streamline-based simulations are utilized to calculate the total UO_3 recovery after leaching, required amount acid volume, and process duration. The simulations model the interactions between reagent and the uranium mineral, assuming simplified chemical kinetics of dissolution. The streamline-based approach simplifies the complex 3D numerical problem into a set of 1D numerical resolutions along the streamlines. By assuming constant average rock properties, ore grade, flow velocity, and porosity within the studied domain, this work has derived a one-dimensional analytical solution for the chemical concentration distribution along the streamlines.

The analytical solution is compared with the one-dimensional numerical solution obtained along streamlines. The results are both qualitatively and quantitatively very similar. The main advantage of the analytical solution is its independence from the computational grid, making it faster than the numerical solution, with improvements of speed ranging from 3.5 to 9 times (depending on the mesh size). In contrast, the numerical solution requires a grid of at least 500 nodes per streamline to reach convergence. We performed a comparative analysis of acid consumption, solid, and dissolved uranium mineral along streamlines for both the analytical and numerical solutions. The relative difference in the total uranium in ore, which is the sum of solid and dissolved uranium, between the analytical and numerical solutions is $<2.5\%$. However, the analytical solution assumes constant rock and ore properties, flow rate, and porosity, which is a limitation not encountered in the numerical resolution.

Then, we compared the analytical and numerical streamline-based approaches with 3D modeling results on a hexagonal well pattern, using 15,600 streamlines from injectors to producers and two mesh sizes: $93 \times 100 \times 40$ and $186 \times 200 \times 40$ nodes for the 3D simulation. The computation was performed on an Intel core i9-9900K processor with a clock speed of 3.6 GHz, and 32 GB of RAM. The streamline numerical solutions were much faster than the 3D solutions, requiring 70 and 440 times less computation time for multicore parallelization and simple-core explicit method, respectively. When we quadrupled the mesh size, the computational time increased by 5.5 to 6 times.

Streamline simulation can reduce the computation time by a factor ranging between hundred and thousand, depending on the computational grid. Although the analytical solution can only be used to quickly predict the process of uranium mining, the numerical study along the streamlines has a significant advantage in terms of calculation time compared to other methods. These faster simulation approaches pave the way for online exploitation simulation, better recovery, and less consumption of acid reagent during the exploitation of ore deposits mined using In-Situ Leaching methods by accounting for rapid changes in exploitation conditions.

Author contributions

Ideas and concepts, M.K., M.T., N.S., and J.-J.R.; methodology design A.K., M.T., and J.-J.R.; software developments and tests, M.K., D.A. and N.S.; analytical modeling, J.-J.R.; case study, M.K., D.A., N. S. and M.T.; original draft manuscript, M.K., D.A. and M.T.; writing-review and manuscript editing, J.-J.R.; visualization, M.K., N.S. and J.-J.R.; project supervision, M.T.; funding acquisition M.T., and A.K. All authors have read and approved the final manuscript.

Funding

The work was supported and partially financed by the Ministry of Science and Higher Education of the Republic of Kazakhstan through grant AP09260105.

Declaration of Competing Interest

The authors declare no conflict of interest.

Acknowledgments

The authors would like to express their gratitude to the anonymous reviewers for their constructive suggestions and improvements, as well as to the editors for their hard work on this paper. We also extend our thanks to Al-Farabi Kazakh National University, Satbayev University, and University of Lorraine for their support. The authors thanks go to Frederic Taylor for proofreading the English version of this article.

References

Aizhulov, D., Tungatarova, M., Kaltayev, A., 2022. Streamlines based stochastic methods and reactive transport simulation applied to resource estimation of roll-front uranium deposits exploited by in-situ leaching. Minerals 12, 1209. https://doi.org/10.3390/min12101209.

Alhashmi, Z., Blunt, M.J., Bijeljic, B., 2015. Predictions of dynamic changes in reaction rates as a consequence of incomplete mixing using pore-scale reactive transport modeling on images of porous media. J. Contam. Hydrol. 179, 171–181 (ISSN: 1873-6009).

Alibayeva, K.A., Tungatarova, M.S., Bibossinov, A.Zh., Kuldzhabekov, A.B., Kaltayev, A., 2009. Study of uranium extraction process by the in-situ leaching method. Drilling Oil and Gas, Quarterly AGH 26 (1–2), 55–61.

Alibayeva, K.A., Kulzhabekov, A.B., Kaltaye, A., 2010. The modeling of uranium extraction process by the in situ leaching method. Drilling Oil-Gas AGH 27 (1–2), 49–57.

Batycky, R.P., Blunt, M.J., Thiele, M.R., 1997. A 3D field-scale streamline-based reservoir simulator. SPE Reserv. Eng. 12 (4), 246–254. https://doi.org/10.2118/36726-PA.

Bear, J., 2014. Dynamics of Fluids in Porous Media. Dover Publications Inc., New York, NY, USA (757 p).

Bhargava, S.K., Ram, R., Pownceby, M., Grocott, S., Ring, B., Tardio, J., Review, L.J., 2015. A review of acid leaching of uraninite. Hydrometallurgy 151, 10–24. https://doi.org/10.1016/j.hydromet.2014.10.015.

Bommer, M.P., Schechter, R.S., 1979. Mathematical modeling of in-situ uranium leaching. SPEJ 19, 393–400.

Bruneton, P., Cuney, M., 2016. Geology of uranium deposits. Uranium Nucl. Power 2, 11–52. https://doi.org/10.1016/B978-0-08-100307-7.00002-8.

Chang, K., Constantinescu, G., Park, S., 2006. Analysis of the flow and mass transfer processes for the incompressible flow past an open cavity with a laminar and a fully turbulent incoming boundary layer. J. Fluid Mech. 561, 113–145. https://doi.org/10.1017/S0022112006000735.

Collet, A., Regnault, O., Ozhogin, A., Imantayeva, A., Garnier, L., 2022. Three-dimensional reactive transport simulation of Uranium in situ recovery: large-scale well field applications in Shu Saryssu Bassin, Tortkuduk deposit (Kazakhstan). Hydrometallurgy 211, 105873. https://doi.org/10.1016/j.hydromet.2022.105873.

Cordes, C., Kinzelbach, W., 1994. Continuous groundwater velocity fields and path lines in linear, bilinear and trilinear finite elements. Water Resources. Res. 30 (4), 965–973.

Cox, J.D., Wagman, D.D., Medvedev, V.A., 1984. CODATA Key Values for Thermodynamics. Hemisphere Publishing Corp, New York (1).

Crane, M.J., Blunt, M.J., 1999. Streamline-based simulation of solute transport. Water Res. Res. 35, 3061–3078 (ISSN: 0043-1397).

CUDA, 2013. C Programming Guide, 214p. www.nvidia.com.

Danaev, N.T., Korsakova, N.K., Penkovskij, V.I., 2005. Mass Transfer in Near-Wellbore Zone and electromagnetic formation logging. Kazakh, National University, Almaty in Russian. (208p).

Darcy, H., 1856. Les Fontaines Publiques de la Ville de Dijon. Dalmont, Paris, 657p. https://gallica.bnf.fr/ark:/12148/bpt6k624312.image, 657p.

Datta-Gupta, A., King, M.J., 1995. A semi-analytic approach to tracer flow modeling in heterogeneous permeable media. Adv. Water Resour. 18 (1), 9–24.

Datta-Gupta, A., King, M.J., 2007. Streamline simulation: theory and practice. Society of Petroleum Engineers (SPE). https://doi.org/10.2118/9781555631116, 404p.

Faraji, F., Alizadeh, A., Rashchi, F., Mostoufi, N., 2020a. Kinetics of leaching: a review. Rev. Chem. Eng. 38, 1–35. https://doi.org/10.1515/revce-2019-0073.

Faraji, F., Alizadeh, A., Rashchi, F., Mostoufi, N., 2020b. Kinetics of leaching: a review. Rev. Chem. Eng. 38, 1–35. https://doi.org/10.1515/revce-2019-0073.

Gerritsen, M.G., Löf, H., Thiele, M.R., 2009. Parallel implementations of streamline simulators. Comput. Geosci. 13 (1), 135–149.

Golubev, V.S., Grabovnikov, V.A., Krichevec, G.N., 1978. On the dynamics of in-situ leaching of minerals based on mathematical modeling, Mathematical and physical modeling of ore-forming processes. In: O dinamike podzemnogo vyshhelachivanija poleznyh iskopaemyh na osnove matematicheskogo i fizicheskogo modelirovanija., Matematicheskoe i fizicheskoe modelirovanie rudo-obrazujushhih processov. GIGHS, Moskva, pp. 122–142 (in Russian).

Grenthe, I., Fuger, J., Konings, R.J.M., Lemire, R.J., Muller, A.B., Nguyen-Trung, C., Wanner, H., 2004. Chemical Thermodynamics of Uranium. OECD Nuclear Energy Agency, Data Bank, N.E.A, Issy-les-Moulineaux (France), 736p. https://www.oecd-nea.org/upload/docs/application/pdf/2019-12/uranium.pdf.

Gromov, B.V., 1978. Introduction to Chemical Technology of Uranium [VVedenie V Himicheskuyu Tehnologiyu Urana]. Atomizdat, Moscow, Russia, 326p. (In Russian).

International Atomic Energy Agency, 2009. World Distribution of Uranium Deposits (UDEPO) with Uranium Deposit Classification. Nuclear Fuel Cycle and Materials Section; International Atomic Energy Agency, Vienna, Austria, p. 117.

Kancel, A.A., 2008. Mathematical modeling of the dynamics of the in-situ leaching process in a heterogeneous ore-bearing layer. Ph.D. Thesis. Lomonosov MSU, Moscow, Russia, 127 p. (in Russian). https://cs.msu.ru/sites/cmc/files/theses/201003-kaa.pdf.

King, M.J., Datta-Gupta, A., 1998. Streamline simulation: a current perspective. In Situ 22 (1), 91–140.

Kuljabekov, A., 2014. Model of Chemical leDaching with Gypsum Sedimentation in Porous Media. Ph.D. Thesis. Univ. Lorraine, Nancy, France & Al Farabi, Almaty, Kazakhstan, 111p. https://hal.univ-lorraine.fr/tel-02075294/file/DDOC_T_2014_0369_KULJABEKOV.pdf.

Kurmanseiit, M.B., Tungatarova, M.S., Kaltayev, A., Royer, J.J., 2022. Reactive transport modeling during uranium in situ leaching (ISL): the effects of ore composition on mining recovery. Minerals 12, 1340–1361. https://doi.org/10.3390/min12111340.

Li, Y., Kawashima, N., Li, J., Chandra, A.P., Gerson, A.R., 2013. A review of the structure, and fundamental mechanisms and kinetics of the leaching of chalcopyrite. Adv. Colloid Interf. Sci. 197-198, 1–32. https://doi.org/10.1016/j.cis.2013.03.004.

OECD, 2008. Uranium 2007: Resources, Production and Demand; NEA #6345. OECD, Boulogne-Billancourt, France.

OECD, 2020. Uranium 2020: Resources, Production and Demand; NEA #7551. OECD, Boulogne-Billancourt, France.

Oladyshkin, S., Royer, J.J., Panfilov, M., 2008. Effective solution through; the streamline technique and HT-splitting for the 3D dynamic analysis of the compositional flows in oil reservoirs. Transp. Porous Media 74 (3), 311–329.

Panfilov, M., Uralbekov, B., Burkitbayev, M., 2016. Reactive transport in the underground leaching of uranium: asymptotic analytical solution for multi-reaction model. Hydrometallurgy 160, 60–72. https://doi.org/10.1016/j.hydromet.2015.11.012.

Peng, X., Du, Z., Liang, B., Qi, Z., 2009. Darcy-stokes streamline simulation for the Tahe-fractured reservoir with cavities. Paper SPE 107314-PA. SPE J. 14 (03), 543–552. https://doi.org/10.2118/107314-PA.

Penkovski, V.I., Rybakova, S.T., 1989. Numerical model of mass transfer process at underground leaching. Continuum dynamics: Institute of Hydrodynamics 81–92.

Penkovskij Ben Simon, R., Thiry, M., Schmitt, J.M., Lagneau, V., Langlais, V., Bélières, M., 2014. Kinetic reactive transport modelling of column tests for uranium in situ recovery (ISR) mining. Appl. Geochem. 51, 116–129. https://doi.org/10.1016/j.apgeochem.2014.09.014.

Pollock, D.W., 1988. Semi-analytical computation of path lines for finite-difference models. Ground Water 26 (6), 743–750.

Press, W.H., Teukolsky, S.A., Vetterling, W.T., Flannery, B.P., 2007. Numerical Recipes: The Art of Scientific Computing, 3rd ed. Cambridge University Press, New York. (1193p., ISBN 0-521-88068-8).

Prévost, M., Edwards, M.G., Blunt, M.J., 2001. Streamline tracing on curvilinear structured and unstructured grids, paper SPE 66347. In: Proc. of the SPE Reservoir Simulation Symposium, Houston, TX. https://doi.org/10.2118/66347-MS, 14p.

Regnault, O., Lagneau, V., Fiet, N., 2015. 3D reactive transport simulations of uranium in situ leaching: forecast and process optimization. In: Merkel, B., Arab, A. (Eds.), Uranium - Past and Future Challenges. Springer, Cham.: Cham, Switzerland, pp. 725–730. https://doi.org/10.1007/978-3-319-11059-2_83.

Steefel, C.I., DePaolo, D.J., Lichtner, P.C., 2005. Reactive transport modeling: an essential tool and a new research approach for the Earth sciences. Earth Planet. Sci. Lett. 240, 539–558. https://doi.org/10.1016/j.epsl.2005.09.017.

Thiele, M.R., 2001. Streamline Simulation. 6th Int. Forum on Reservoir Simulation, Sept. 3rd -7th. Schloss Fuschl, Austria, 24p.

Thiele, M.R., Batycky, R.P., Fenwick, D.H., 2010. Streamline simulation for modern reservoir-engineering workflows. J. Pet. Technol. 62 (01), 64–70.

Torrero, M.E., Baraj, E., Pablo, J., Giminez, J., Casas, I., 1997. Kinetics of corrosion and dis- solution of uranium dioxide as a function of pH. In. J. Chem. Kinet. 29, 261–267.

Uranium Production by Country, 2022. 2022. Available online. https://worldpopulationreview.com/country-rankings/uranium-production-by-country (accessed on 1 October 2022).

Wen, T., Thiele, M.R., Ciaurri, De, Aziz, K., Ye, Y., 2014. Waterflood management using two-stage optimization with streamline simulation. Comput. Geosci. 18 (3), 483–504.

Zheng, C., Wang, P.P., 1999. MT3DMS: A Modular Three-Dimensional Multispecies Transport Model for Simulation of Advection, Dispersion, and Chemical Reactions of Contaminants in Groundwater Systems; Documentation and User's Guide. Vicksburg, MS, USA, Engineer Research and Development Center, 220p. https://hdl.handle.net/11681/4734, 220p.